International Journal of Research
Available at https://edupediapublications.org/journals

e-ISSN: 2348-6848
p-ISSN: 2348-795X
Volume 04 Issue 13
October 2017

Weighted Guided Image Filter for Smoothing and Haze Removal

S.Aruna Kumari[1], K.Rajasekhar[2]

Research Associate ,Dept. of Electronics and Communication Engineering ,UCEK(A), JNTUK,Kakinada, Andhra Pradesh, India[1]

Assistant Professor ,Dept. of Electronics and Communication Engineering ,UCEK(A), JNTUK,Kakinada, Andhra Pradesh, India[2]

Abstract:

Most applications in computer vision and computer graphics involve image filtering to suppress and extract content in images. In this applications Edge preserving smoothing is the concerned area. There are different edge preserving filters. Those are global filters and local filters. Local filters like guided filter is very simple but it produces halo arifacts. Global filters like Weighted least square filter preserve sharp edges but have high computational complexity. So we proposed Weighted guided filter by incorporating edge aware weighing into the guided filter. It preserves sharp edges like global filters and it is very simple as local filters. Due to its simplicity it is used in different applications like single image haze removal. Remote sensing images such as satellite and underwater images are widely used in various fields of computer vision. But due to fog, mist and various aerosals in the atmosphere their contrast get reduced. So here for single image haze removal weighted guided image filter is used.

Keywords:
Edge-preserving smoothing, weighted guided image filter, edge-aware weighting, haze removal

1. Introduction

Generally edges provide an effective and expressive simulation for human visual perception. So it is important to preserve sharp edges in image smoothing. There are two types of edge preserving smoothing techniques. Those are global optimisation filters and local optimisation filters. The global optimisation filters in [1], [2], [3], and [4]. The performance criterion consists of data term and regularisation term. The data term measures fidelity of reconstructed image with respect to the image to be filtered while the regularization term provides the smoothness level of the reconstructed image. Global optimisation filters provides excellent quality in preserving sharp edges but have high computational complexity. The other type is local filters. Those are bilateral filter (BF) [5], its extension in gradient domain [6], trilateral filter [7], and their accelerated versions [8], [9], [10] as well as guided image filter (GIF) [11]. Local filters are simple compared to global filters but local filters can not preserve sharp edges like global filters. So it is necessary to design a new filter which preserves the sharp edges like global filter and is as fast as local filters.

An interesting algorithm named weighted guided image filtering scheme is proposed in this paper by combining the edge-based weighting scheme along with guided image filtering. Edge based weighting scheme is calculated by using local variance in a guidance image with box filter of 3×3 window. This local variance scheme of one individual pixel is normalized by all pixels local variance in guidance image. The acquired normalized weights of all pixels are then adapted to design WGIF. WGIF helps to avoid halo artifacts in accurate manner for excellent visual quality. The intricacy of WGIF is same as GIF. Fog formation is due to attenuation and airlight. Attenuation reduces the contrast and air light increases the whiteness in the scene. Proposed algorithm uses bilateral filter for the estimation of air light and recover scene contrast. Qualitative and quantitative analysis demonstrate that proposed algorithm performs well in comparison with prior state of the art algorithms. Proposed algorithm is independent of the density of fog and does not require user intervention. It can handle colour as well as gray images. Proposed algorithm achieves better results than other existing algorithms. Proposed algorithm does not require any user intervention and is applicable for colour as well as gray images.

2. Previous work

2.1 Explicit Weighted Average Filters:

The bilateral filter [5] is perhaps the simplest and most intuitive one among explicit weighted-average filters. It computes the filtering output at each pixel as the average of neighboring pixels, weighted by the Gaussian of both spatial and intensity distance. The bilateral filter smooths the image while preserving edges but it produces gradient reversal artifacts. These artifacts exists when a pixel found few simiar pixels around it. In this case results may produce unwanted profile around edges that may cause uncertainity.

2.2 Implicit Weighted Average filters:

Implicitly filtering of an image by an inverse matrix is nothing but optimizing the quadratic cost function and solving a linear system. The Weighted least squares filter [3] adjusts the matrix affinities according to the image gradients and produces halo free edge preserving smoothing.

2.3 Guided filter:

The task of edge-preserving smoothing is to molder an image I into two parts as follows

$$Z(p) = R(p) + e(p) \quad (1)$$

where R is a reconstructed image formed by uniform regions with sharp edges, e is noise or texture, and p(=(x , y)) is a position. R and e are called base layer and detail layer respectively. One type of local edge preserving smoothing filter is BF [5]. BF [5] is very simple but it produce gradient reversal artifacts and the results may produce undesired profiles around edges. So to overcome this problem GIF was introduced in[11]. In the GIF [11] guidance image G is used which could be identical to the image Z. R is a linear transform of G in the window Ως (p').

$$R(p) = c_{p'}G(p) + d_{p'}\, p \in \Omega_{\varsigma}(p') \quad (2)$$

Ως (p') is a square window centred at pixel of radius ς. $c_{p'}$ and $d_{p'}$ are two constants in the window Ως(p').

To determine the linear coefficients $(c_{p'}, d_{p'})$ a constraint is added to Z and R as in Equation (1). The values of $c_{p'}$ and $d_{p'}$ are then obtained by minimizing a cost function $E(c_{p'}, d_{p'})$ which is defined

$$E(c_{p'}, d_{p'}) = \sum_{p \in \Omega_{\varsigma}} \left[\left(c_{p'}G(p) + d_{p'} - Z(p)\right)^2 + \lambda c_{p'}^2 \right] \quad (3)$$

Where λ is a regularization parameter .The value of λ is fixed in GIF[11]. So halo artifacts are occurred and can't be removed when this filter is applied for smoothing of the image. While in global filters it is varied. So halo artifacts avoided.

3. Proposed Weighted Guided Filter

3.1Edge Aware Weighing:

Let *G* be a guidance image

$$\Gamma_G(p') = \frac{1}{M} \sum_{p=1}^{M} \frac{\sigma_{G,1}^2(p') + \alpha}{\sigma_{G,1}^2(p) + \alpha} \quad (4)$$

where α is a small constant and its value is selected as $(0.001{*}D)^2$ where D is the dynamic range of the input image.

In the computation Of $\Gamma_G(p')$ all pixels in the guidance image are used. If p' is at an edge the value of $\Gamma_G(p')$ is usually larger than1 and smaller than 1 if $p'$is in a smooth area. Thus from this we can say that larger weights are assigned to pixels at edges than those pixels in flat areas by using the Weight$\Gamma_G('p)$inEquation(4)

Fig 1.Where (a) is the input image (b) weighing of input image.

3.2 Proposed method by combining both GIF and An Edge-Aware Weighting:

Same as the GIF, the key assumption of the WGIF is a local linear model between the guidance image *G* and the filtering output *R* as in Equation (2). This model provides that the output *R* has an edge only if the guidance image *G* has an edge.

The proposed weighting $\Gamma_G(p')$in Equation (5) is integrated into the cost function $E(c_{p'}, d_{p'})$ in Equation (3). As such the solution is obtained by minimizing the difference between the image to be filtered *X* and the filtering output R while maintaining the linear model (2), i.e., by minimizing a cost function $E(c_{p'}, d_{p'})$ which is defined as

$$E = \sum_{p \in \Omega_{\varsigma}} \left(\left(c_{p'}G(p) + d_{p'} - Z(p)\right)^2 + \frac{\lambda}{\Gamma_G(p')} c_{p'}^2 \right) \quad (5)$$

The values of $c_{p'}$ and $d_{p'}$ are computed as

$$c_{p'} = \frac{\mu_{G\odot Z,\varsigma}(p') - \mu_{G,\varsigma}(p')\mu_{Z,\varsigma}(p')}{\sigma_{G,\varsigma}^2(p') + \dfrac{\lambda}{\Gamma_G(p')}} \quad (6)$$

$$d_{p'} = \mu_{Z,\varsigma}(p') - b_{p'}\mu_{G,\varsigma}(P') \quad (7)$$

where ⊙ is the element by element product of two matrices.

$\mu_{G\odot Z,\varsigma}(p'), \mu_{G,\varsigma}(P')$and $\mu_{G,\varsigma}(P')$ are mean values of $G\odot Z$,G and X respectivey.

e-ISSN: 2348-6848
p-ISSN: 2348-795X
Volume 04 Issue 13
October 2017

The final value of $R(p)$ can be calculated as

$$R(p)=\bar{c}_pG(p)+\bar{d}_p \qquad (8)$$

Where $\bar{b}_p$ and $\bar{c}_p$ are mean values of $b_{p'}$ and $c_{p'}$ in the window computed as

$$\bar{b}_p=\frac{1}{|\Omega_\zeta(p)|}\sum_{p'\in\Omega_\zeta(p)}c_{p'};\bar{c}_p=\frac{1}{|\Omega_\zeta(p)|}\sum_{p'\in\Omega_\zeta(p)}d_{p'} \qquad (9)$$

Where $|\Omega_\zeta(p)|$ is the cardinality of $\Omega_\zeta(p)$

The images I and G are assumed to be the same for easy analysis. Consider the case that the pixel p' is at an edge. The value of $\Gamma_G(p')$ s usually much larger than 1. $c_{p'}$ in the WGIF is closer to 1 than $c_{p'}$ in the GIF [11]. Then this implies that the sharp edges are preserved better by the WGIF compared to the GIF[11].

Comparison of Guided filter and WGF:

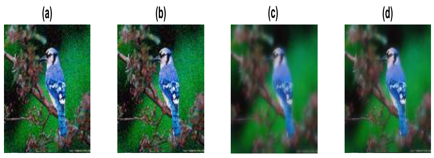

Fig 2. (a) input image (b) guidance image (c) GF output (d) WGF output

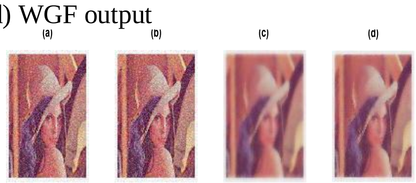

Fig 3. (a) input image (b) guidance image (c) GF output (d) WGF output

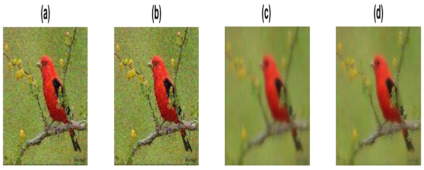

Fig 4. (a) input image (b) guidance image (c) GF output (d) WGF output

Table 1

	PSNR		MSE	
	WGF	GF	WGF	GF
Image 1	20.98	19.56	0.0080	0.0011
Image 2	21.05	19.26	0.0108	0.0168
Image 3	21.88	20.22	0.0065	0.0095

Table 1:comparison of WGIF and GIF with peak signal to noise ratio and mean square error

3.3 Single Image Haze Removal:

Images of outdoor scenes are usually degraded by turbid medium (*e.g* particles, water droplets) in the atmosphere. Haze, fog and smoke are such phenomena due to atmospheric absorption and scattering. Generally the degraded images lose the contrast and color fidelity. So it is highly desired to remove the haze of the degraded image.Removal of haze can significantly increase the visibility of the scene and correct the color shift caused by the airlight and most computer vision algorithms from low-level image analysis to high-level object recognition, usually assume that the scene radiance is the input image. The model adopted to describe the formulation of haze image is given as [12].

$$I_c(P)=R_c(p)t(p)+A_c(1-t(p)) \qquad (10)$$

where $c \in \{r, g, b\}$ is a color channel index, I_c is the observed intensity R_c is the scene radiance, A_c is the global atmospheric light, and t is the medium transmission describing the portion of the light that is not scattered and reaches the camera.

The first term $R_c(p)t(p)$ is called direct attenuation [13] and it describes the scene radiance and its decay in the medium. The second term $A_c(1-t(p))$ is called airlight. The objective of haze removal is to restore R from the input I. Three major problems to be addressed for single image haze removal in [14] are Halo artifacts, amplification of noise in sky regions, and color fidelity.

Let $\varphi_c(.)$ be a minimal operation along the color channel {r,g,b} and it is defined as

$$A_{\min}(p)=\varphi_c(A_c)=\min\{A_r,A_g,A_b\} \qquad (11)$$

$$I_{\min}(p)=\varphi_c(I_c(p))=\min\{I_r(p),I_g(p),I_b(p)\} \qquad (12)$$

$$R_{\min}(p)=\varphi_c(R_c(p))=\min\{R_r(p),R_g(p),R_b(p)\} \qquad (13)$$

it can be derived from the haze image model in Equation (12) that

$$I_{\min}(P)=R_{\min}(P)t(P)+A_{\min}(1-t(P)) \qquad (14)$$

By using the haze image model in Equation (16), a simplified dark channel is defined as{*r*,*g*,*b*} and it is defined as

$$J^R_{dark}(p)=\psi_\zeta(\varphi_c(R(p))) \qquad (15)$$

Where $\psi_\zeta(R(p))=\min(R(p'))$ and $p'\in\Omega_\zeta(P)$ (16)

is nothing but the minimal of neighbourhood.

Similar to [15], the value of t(p) is assumed to be constant in the neighbourhood. It can be derived from Equation (10) It is worth noting that the initial value of *t (p)* in [15] is given as

$$J^I_{dark}(p)=J^R_{dark}(p)t(p)+A_{\min}(1-t(p)) \qquad (17)$$

Obviously, it is simpler to estimate the initial value of $t(p)$ by using the proposed simplified dark channel.

$$t(P) = 1 - \varphi_c\left(\psi_\varsigma\left(\frac{R_c(P)}{A_c}\right)\right) \quad (18)$$

The value of $A_c(c \in \{r,g,b\})$ is estimated by using $J^I_{dark}(p)$ and $I_c(p)$ in the dark channel the brightest pixels are first selected. The value of $A_c(c \in \{r,g,b\})$ is set as the average intensity of these pixels along each color channel.

The initial value of $t(p)$ is then computed as

$$t(p) = 1 - \frac{31}{32}\frac{J^I_{dark}(p)}{A_c} \quad (19)$$

The estimated transmission map t(p) is filtered by using the WGF with guidance image as luminance component of the haze image.

Finally the scene radiance is recovered by

$$R_c(p) = \frac{I_c(p) - A_c}{t(p)} + A_c; c \in \{r,g,b\} \quad (20)$$

For distance objects a very small amount of haze is left and presence of haze is fundamental cue for human to perceive depth, the small amount of haze left for the distant objects helps preserve the feeling of depth in the dehazed image better.

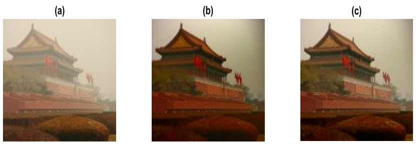

Fig 5: (a) is input haze image (b) is dehazed image by GF (c) is dehazed image by WGF.

4. Conclusion

From the comparison table we can say that the PSNR of WGF is high compared to GIF and the Mean square error is less. From simulation results we can say that the visual quality of WGIF results are better compared to GIF and halo arifacts also avoided. Thus the WGIF preseves sharp edges like global filters and is very simple as GIF. WGIF has ability to provide the local and global smoothing filters advantages and successful to avoid the halo artifacts. Due to its high simplicity it is used in many applications like single image haze removal. In haze removal also WGIF provided the better result compared to GIF. Naturalness of the WGIF is high compared to GIF.

5. References

[1] P. Charbonnier, L. Blanc-Feraud, G. Aubert, and M. Barlaud, "Deterministic edge-preserving regularization in computed imaging," *IEEE Trans. Image Process.*, vol. 6, no. 2, pp. 298–311, Feb. 1997.

[2] L. I. Rudin, S. Osher, and E. Fatemi, "Nonlinear total variation based noise removal algorithms," *Phys. D, Nonlinear Phenomena*, vol. 60, nos. 1–4, pp. 259–268, Nov. 1992.

[3] Z. Farbman, R. Fattal, D. Lischinski, and R. Szeliski, "Edge-preserving decompositions for multi-scale tone and detail manipulation," *ACM Trans. Graph.*, vol. 27, no. 3, pp. 249–256, Aug. 2008.

[4] L. Xu, C. W. Lu, Y. Xu, and J. Jia, "Image smoothing via *L*0gradient minimization," *ACM Trans. Graph.*, vol. 30, no. 6, Dec. 2011, Art. ID 174.

[5] C. Tomasi and R. Manduchi, "Bilateral filtering for gray and color images," in *Proc. IEEE Int. Conf. Comput. Vis.*, Jan. 1998, pp. 836–846.

[6] Z. Li, J. Zheng, Z. Zhu, S. Wu, and S. Rahardja, "A bilateral filter in gradient domain," in *Proc. Int. Conf. Acoust., Speech Signal Process.* Mar. 2012, pp. 1113–1116.

[7] P. Choudhury and J. Tumblin, "The trilateral filter for high contrast images and meshes," in *Proc. Eurograph. Symp. Rendering*, pp. 186–196, 2003.

[8] R. Fattal, M. Agrawala, and S. Rusinkiewicz, "Multiscale shape and detail enhancement from multi-light image collections," *ACM Trans. Graph.*, vol. 26, no. 3, pp. 51:1–51:10, Aug. 2007.

[9] F. Durand and J. Dorsey, "Fast bilateral filtering for the display of highdynamic- range images," *ACM Trans. Graph.*, vol. 21, no. 3, pp. 257–266,Aug. 2002.

[10] J. Chen, S. Paris, and F. Durand, "Real-time edge-aware image processing with the bilateral grid," *ACM Trans. Graph.*, vol. 26, no. 3, pp. 103–111, Aug. 2007.

[11] K. He, J. Sun, and X. Tang, "Guided image filtering," *IEEE Trans. Pattern Anal. Mach. Intell.*, vol. 35, no. 6, pp. 1397–1409, Jun. 2013.

[12] S. G. Narasimhan and S. K. Nayar, "Chromatic framework for vision in bad weather," in *Proc. IEEE Conf. Comput. Vis. Pattern Recognit. (CVPR)*, Jun. 2000, pp. 598–605..

[13] R. T. Tan, “Visibility in bad weather from a single image,” in *Proc. IEEE Conf. Comput. Vis. Pattern Recognit. (CVPR)*, Jun. 2008, pp. 1–8.

[14] x. Lv, W. Chen, and I.-F. Shen, “Real-time dehazing for image and video,” in *Proc. 18th Pacific Conf. Comput. Graph. Appl.*, Sep. 2010, pp. 62–69.

[15] K. He, J. Sun, and X. Tang, “Single image haze removal using dark channel prior,” *IEEE Trans. Pattern Anal. Mach. Intell.*, vol. 33, no. 12, pp. 2341–2353, Dec. 2011. pp. 62–69.

[16] J. Pang, O. C. Au, and Z. Guo, “Improved single image dehazing using guided filter,” in *Proc. APSIPA ASC*, Xi’an, China, 2011, pp. 1–4.